INTERNATIONAL JOURNAL
FOR RESEARCH

IN APPLIED SCIENCE & ENGINEERING TECHNOLOGY

Structural and Dielectric Properties of Ba-Co-Zr Hexagonal Ferrites

Ch. Venkateshwarlu[1], P. Vijaya Bhasker Reddy[2]

[1] *Department of Physics, University College of Science, Saifabad, Osmania University, Hyderabad-500004, Telangana, India.*
[2] *University College for Women, Osmania University Hyderabad-500095,Telangana,India.*

Abstract: Dielectric properties such as dielectric constant (ϵ') and dielectric loss tangent (tan δ) of mixed Ba-Co-Zr ferrites having the compositional formula $BaCo_xZr_xFe_{12-2x}O_{19}$ (where x =0.0, 0.2, 0.4, 0.6, 0.8 and 1.0) were measured at room temperature in the frequency range 1 MHz to 1.8GHz using a 4291B impedance analyser plots of dielectric constant (ϵ') vs. frequency show a normal dielectric behaviour of ferrites. The frequency dependence of imaginary permittivity was found to be abnormal, giving a peak at certain frequency for all mixed Ba-Co-Zr ferrites. A qualitative explanation is given for the composition and frequency dependence of the dielectric constant and dielectric loss tangent.
Keywords: **Structure; Permittivity; Dielectric constant; dielectric loss tangent; Ba-Co-Zr ferrites.**

I. INTRODUCTION

Ferrites materials are being widely used in the devices operating at higher frequencies. The hexagonal ferrites $MFe_{12}O_{19}$ (M=Ba, Sr and Pb) with magneto plum bite structure are important permanent magnetic materials in microwave, small motor and more recently magnetic recording applications [1-4]. These materials have good mechanical, chemical stability. Several cations such as $Cr^{3+}, Al^{3+}, Ga^{3+}$ have been attempted by several researchers[5-8] in order to improve the electrical properties of Ba-hexaferrite. The M-type ferrite crystallizes in a hexagonal structure with 64 ions per unit cell on 11 different symmetry sites. The 24 Fe^{3+} atoms are distributed over five different sites: three octahedral sites one tetrahedral site and one trigonal bipyramidal site. At high frequencies, hexaferrites are considered superior to other magnetic materials because they have low eddy current loss and high electrical resistivity. Hence with a view to the understanding of dielectric phenomena in mixed Ba-Co-Zr ferrites, a systematic study of dielectric properties as a function of composition and frequency was undertaken. The results of the study are presented in this communication.

II. EXPERIMENTAL DETAILS

In the present study of BaM hexagonal ferrites codoped with Co^{2+} and Zr^{4+} (Ba-Co-Zr) having the compositional formula $BaCo_xZr_xFe_{12-2x}O_{19}$ (where x = 0.0, 0.2, 0.4, 0.6, 0.8 and 1.0) were prepared by conventional double sintering method using highly pure $BaCO_3$ (AR 99%), ZrO_2 (AR 99%), CO_3O_4 (AR 99%) and Ferric oxide (Fe_2O_4). The selected samples were pre-sintered at 1000^oC for 10 hrs and last sintering was carried out at 1250^oC for 15 hrs, the sintering atmosphere being air. The XRD analysis is performed to confirm the phase formation of hexa ferrites by Philips Xexpert, which using Co Kα radiation source with λ = 1.7902 A^0. SEM analysis was carried out by LEO-440i microscope. Dielectric properties such as dielectric constant (ϵ') and dielectric loss tangent (tan δ) of mixed Ba-Co-Zr ferrites were measured at room temperature in the frequency range 1 MHz to 1.8GHz using a 4291B impedance analyser plots of dielectric constant (ϵ') vs. frequency show a normal dielectric behaviour of ferrites

III. RESULTS AND DISCUSSION

Figure.1 shows the X-ray diffraction pattern for Ba-Co-Zr hexagonal ferrites. The diffraction patterns confirm the presence of single phase M-type hexa ferrite phase structure. The lattice parameters of the mixed ferrites were calculated from d-spacing and are given in Table 1. It can be experimentally obsevered from the table that the values of lattice parameters, **a** and **c**, continuously increase with the increase of Co and Zr doping concentrations. This can be expected in view of the fact that the ionic radii of 0.82 A^o for the Co^{2+} ions and for the Zr^{4+} ions (0.84 A^o) are more than that of the Fe^{3+} ions (0.64 A^o).
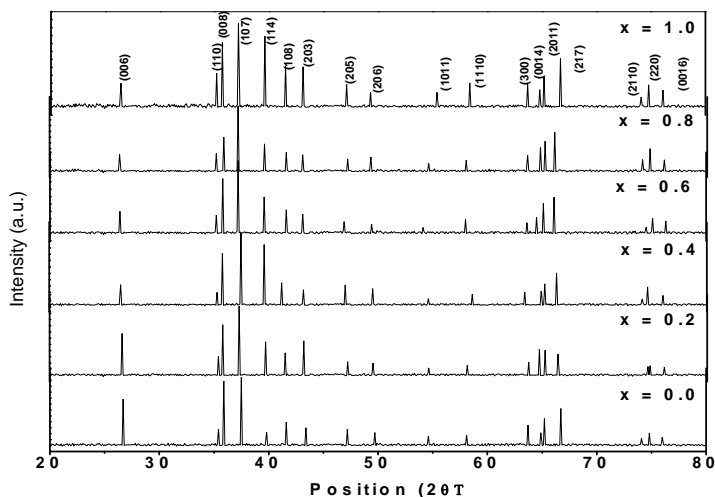
Fig. 1: X-ray diffraction patterns of $BaCo_xZr_xFe_{12-2x}O_{19}$ hexaferrite samples (with x = 0.0, 0.2, 0.4, 0.6, 0.8 and 1.0).

The porosity values of the synthesized samples are calculated by using the formula $P=(1-d/d_x)\times100$, where d is the bulk density and d_x is the x-ray density. The obtained porosity values are given in Table.1. The decrease in porosity indicates that the substituted ions may have causing the densification of the barium hexaferrite matrix. It can be seen that the x-ray density is increasing with increasing content of Co^{2+} and Zr^{4+} in the BaM ferrite. This may be due to the larger ionic sizes of substituents when compared to that of Fe^{3+} ion. Further, the values of bulk density are smaller than the corresponding values of x-ray density. This can be attributed to the existence of pores in the samples.

Table 1: Lattice parameters, porosity values, etc. of Ba-Co-Zr hexagonal ferrites

Sl. No.	Ferrite composition	a(A0)	c (A0)	Volume (Å3)	X-ray density (g/cm3)	Bulk density (g/cm3)	Porosity (%)	Grain size (μm)
1.	BaFe12O19	5.890	23.208	697.266	5.271	4.544	14	5
2.	BaCo0.2Zr0.2Fe11.6O19	5.891	23.213	697.654	5.285	4.653	12	6
3.	BaCo0.4Zr0.4Fe11.2O19	5.893	23.224	698.458	5.322	4.896	8	8
4.	BaCo0.6Zr0.6Fe10.8O19	5.897	23.243	699.979	5.336	4.962	7	10
5.	BaCo0.8Zr0.8Fe10.4O19	5.903	23.267	702.128	5.348	5.012	6	7
6.	BaCo1.0Zr1.0Fe10O19	5.905	23.271	702.725	5.426	5.127	5	4

Fig.2 shows the SEM micrographs of Ba-Co-Zr hexa ferrites. It can be seen from the micrographs that the morphology of particles is similar and they are largely agglomerated. The average grain size of the samples calculated from line intercept method from SEM

micrographs is in the range of 4 to 10 μm. With the increase Co-Zr doping up to x=0.6 the average grain size for all the samples increases and with the further increase of x, grain size decreased.
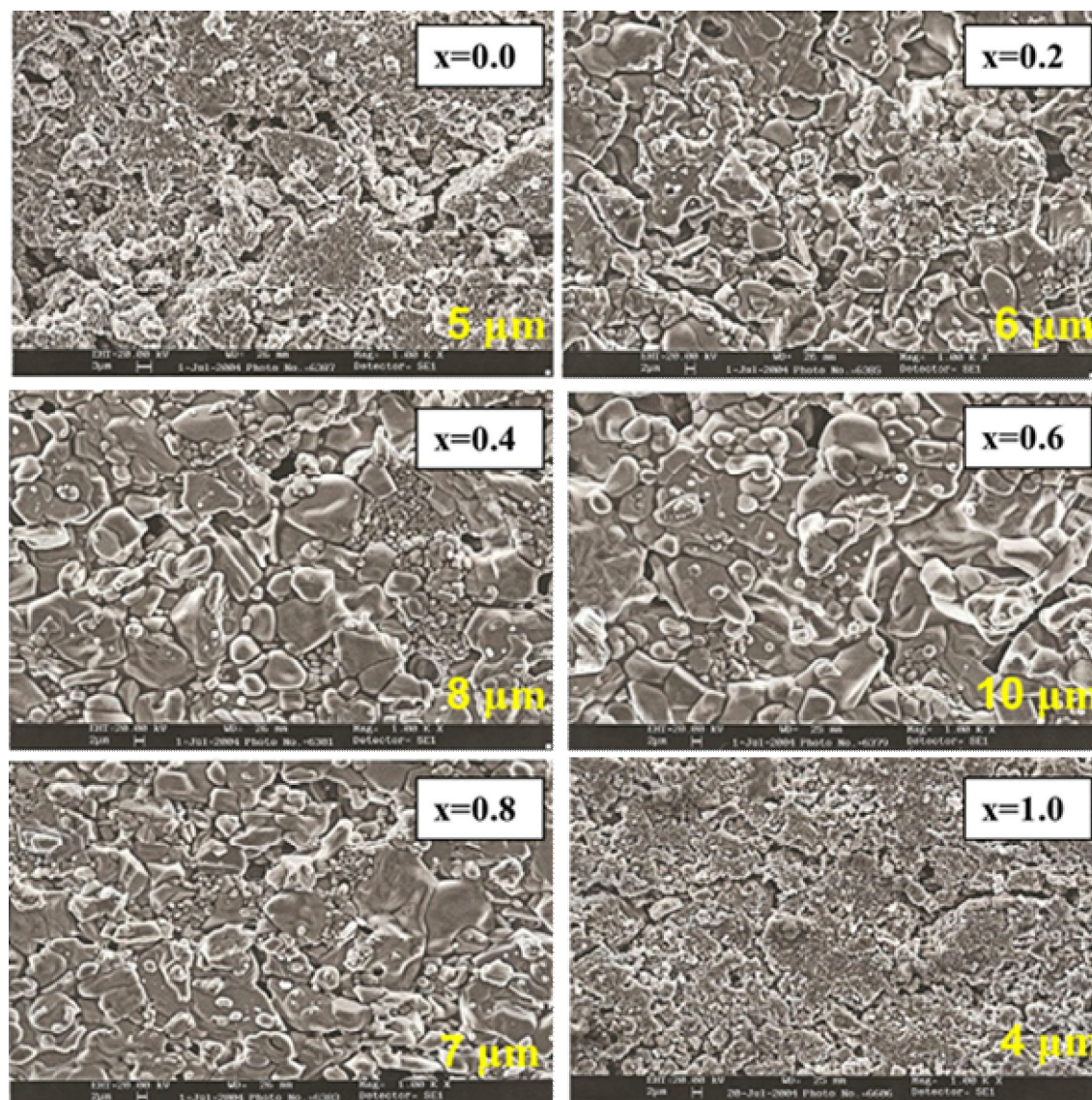

Fig. 2.: SEM micrographs of $BaCo_xZr_xFe_{12-2x}O_{19}$ hexagonal ferrite samples

The frequency variation of real and imaginary parts of relative permittivity (ε' & ε'') for all the samples under investigation was measured and obtained results are plotted in Figs.3 & 4. It can be seen from the figures that the value of ε' remains constant upto a frequency 1 GHz and increases further increase of frequency. In all the samples a resonance and anti resonance peak was observed above 1 GHz. This behavior can be explained in the following way: The ε' remains constant in the frequency range from 1 MHz to 1 GHz due to the hoping electrons will not follow the external applied field. Whereas the increase of ε' above 1GHz is may be due to the following of hopping electrons in the external field. When the hoping frequency of the electrons is equal to that of the external applied electric field, a peak is obtained in the dielectric constant and it is called as the dielectric resonance. Similar behavior was observed by several investigators in many ferrite systems [9-12].

A dielectric constant and dielectric loss for all the investigated samples at 1 MHz is tabulated in Table 2. It is observed that with an increase of x from 0 to 1.0, the values of dielectric constant (ε') decreased from 33 to 6 at 1MHz. This is due to the formation of Fe^{2+} ions from Fe^{3+} ions at high sintering temperature of 1250°C. The dielectric constant in ferrites depends on space charge polarization and charge formation at grain boundaries. The electron hopping between Fe^{2+} ions and Fe^{3+} ions leads to conductivity and dielectric

polarization in ferrites [13]. Researchers have reported the formation of Fe^{2+} ions from Fe^{3+} ions in the high temperature synthesis of ferrites [14-17].

A sample with x = 0.0, i.e., an undoped $BaFe_{12}O_{19}$ is showing large value of dielectric constant compared to doped one which is due to the fact that undoped sample posses large number of Fe^{3+} ions. Thus polarization is enhanced resulting in an increase
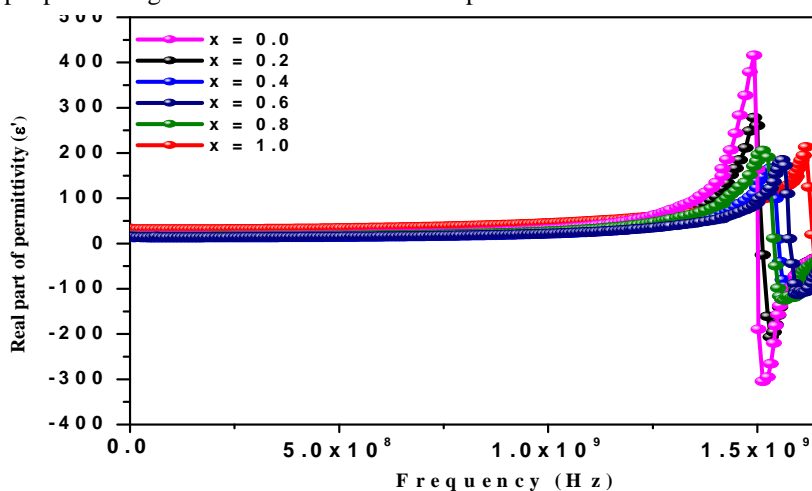

Fig 3: Frequency dependence of real (ε') part of relative permittivity
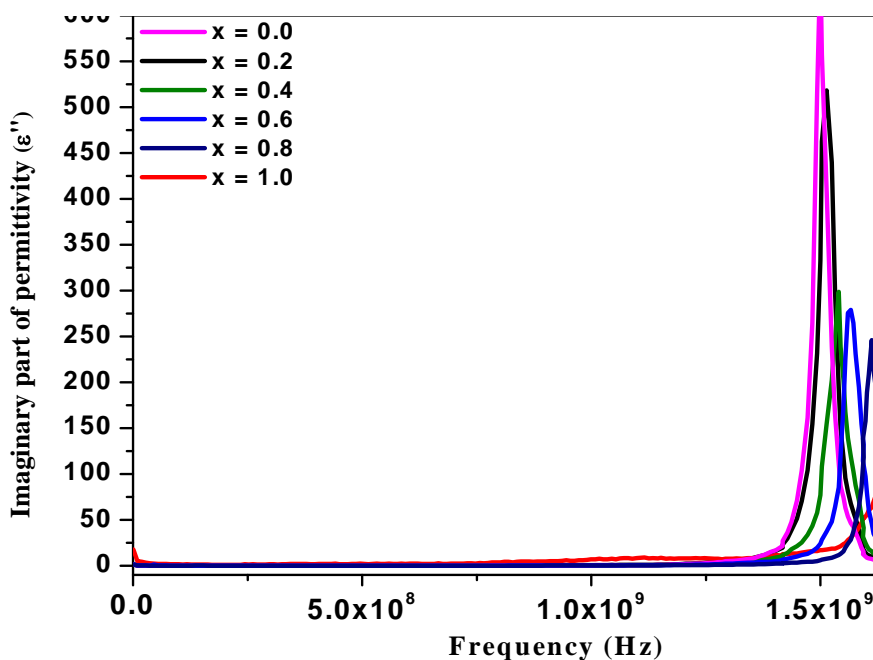for Co-Zr doped $BaFe_{12}O_{19}$

Fig4 : Frequency dependence of imaginary (ε") part of relative permittivity
for Co-Zr doped $BaFe_{12}O_{19}$

of both ε' and ε" in sample x = 0.0. The mechanism of complex permittivity can be discussed in this way: Substitution of ions of ferrites with different valences causes defects in the lattice either in the form of vacancies or in the form of interstitials. In this composition, Co^{2+} and Zr^{4+} ions are substituted to $BaFe_{12}O_{19}$ containing Fe^{3+} ions. Some of the Fe^{3+} ions are replaced with lower valence ions (Co^{2+}) creating anionic vacancies and higher valence Zr^{4+} ions will result in cationic vacancies. These vacancies created, along with the preferential site occupancy of Co^{2+} and Zr^{4+} ions, will change the resistivity of the material and modify the hopping conduction. The electron hopping in cationic and anionic vacancies will increase dielectric losses. The formation of defects and ionic vacancies results in bonding of the material becoming more ionic in nature, thereby increases permittivity.

Table 2: Data of dielectric and magnetic properties of Co-Zr doped $BaFe_{12}O_{19}$ hexagonal ferrites

S. No.	Composition	ε'	ε"	Resonance frequency (GHz)
1	$BaFe_{12}O_{19}$	33	5.4	1.3
2	$BaCo_{0.2}Zr_{0.2}Fe_{11.6}O_{19}$	22	4.5	1.31
3	$BaCo_{0.4}Zr_{0.4}Fe_{11.2}O_{19}$	18	4.1	1.32
4	$BaCo_{0.6}Zr_{0.6}Fe_{10.8}O_{19}$	15	3.8	1.35
5	$BaCo_{0.8}Zr_{0.8}Fe_{10.4}O_{19}$	11	3.2	1.36
6	$BaCo_{1.0}Zr_{1.0}Fe_{10.0}O_{19}$	6	2.9	1.4

The dielectric loss (ε") has been measured on all the samples in the frequency range of 1 MHz to 1.8 GHz and obtained results are plotted in Fig.4. It can be seen from the figure that the value of ε" is small and remains almost constant from 1 MHz to 1GHz. The ε" value increases with an increase of frequency from 1 GHz to 1.8 GHz and finally shows a peak around 1.5 GHz. The variation of dielectric loss with frequency may be explained similar to that of ε' variation with frequency.

Dielectric loss of polycrystalline ferrite ceramics results from the lag in polarization versus the alternating electric field, which has several contributors, such as (i) electron polarization losses, (ii) ion vibration and deformation losses, and (iii) ionic migration losses (including DC conduction loss and ionic jump and dipole relaxation losses). The electron polarization losses are responsible for absorption and color in the visible spectrum. The ion vibration and deformation losses are only of importance in the infrared and not a major concern for frequencies below ~10 GHz. Therefore, the main contribution to dielectric losses of ferrite ceramics would be the ion migration losses, where conduction losses are more significant than other losses. The presence of impurities and the imperfection in the ferrite structure lead to high conductivity and high

losses [18]. However, the most significant contribution to dielectric loss comes from the conduction loss due to the electron hopping between Fe^{2+} and Fe^{3+} ions, especially at low frequencies.

IV. CONCLUSIONS

The frequency of real and imaginary parts of permittivity (ε' & ε") for all the samples under investigation was measured in the frequency range of 1MHz to 1.8GHz. It is observed that with an increase of composition (x) from 0 to 1.0 the values of ε' decreased from 33 to 6 at 1MHz. The ε" value increases with an increase of frequency from 1GHz to 1.8 GHz and finally shows a peak around 1.5GHz. The dielectric losses are in the range of 5.4 to 2.9.

V. ACKNOWLEDGEMENT

REFERENCES

[1]   W.Eerenstein, N.D.Mathur, J.F. Scott, Nature. 442 (2006) 759.
[2]   Muhammad Naeem Ashiq,Muhammad Javed Iqbal,Iftikhar Hussain Hussain Gul, J.Alloys and Compounds 487 (2009) 341-345.
[3]   S.H. Sun, H.Zeng. J.Am. Chem. Soc. 124 (2002) 8204.
[4]   M. H.Sousa, F.A. Tourinho, J.Phys.Chem. B 105 (2001) 1168.
[5]   M.J. Iqbal, M.N.Ashiq, Scripta Mater, 56 (2007) 145.
[6]   S.Thompson, N. Shirtcliffe, E.S.O.Keefe,S. Appleton, C.C. Perry, J.Magn.Magn. Mater,292 (2005) 100.
[7]   Q.Q.Fang,H.Cheng,K.Huang,J.Wang,R.Li,Y.Jiao, J.Magn. Magn.Mater. 294 (2005) 281.
[8]   G.Surig, K.A.Hempel, D. Bonnenber, Appl. Phys.Lett.74 (1999) 2513
[9]   A. M., B.K. Shaikh, S. S. Bellad Chougule, J.Magn.Magn.Mater., 195 (1999) 384.
[10] A. Verma, T.C.Goel, R.G.Menditratta, M.I.Alam, Mater.Sci.Eng.B., 60 (1999) 156.
[11] A. Verma, T. C. Goel, R. G. Mendiratta, J. Magn. Magn. Mater., 195 (2000) 274.
[12] V. R. K. Murthy, J. Shobhanadri, Phys. Status. Solidi. A., 36 (1976) 133.
[13] A.M. Abdeen, J.Magn.Magn.mater., 192 (1999) 121.

[14] N. Gupta, M.C.Dimri, S.C.Kashyap and D.C.Dubey, Ceramics International, 31 (2005) 171.

[15] L.G. Van Uitert, J.Chem.Phys., 23 (1995) 1883.

[16] A. Verma, R. Chatterjee, J. Magn. Magn. Mater., 306 (2006) 313.J.M. Brownlow, J.Appl. Phys., 29(1958) 373.

[17] . Kingery, H.K. Bowen, D.R. Uhlmann, Introduction to Ceramics, second ed., John Wiley & Sons, New York, 1976, pp. 913–945.

INTERNATIONAL JOURNAL FOR RESEARCH

IN APPLIED SCIENCE & ENGINEERING TECHNOLOGY

Call : 08813907089 ⊙ (24*7 Support on Whatsapp)